Manipulating terahertz electromagnetic induced transparency through parallel plate waveguide cavities

Lin Chen,[a] Jiaming Xu, Chunmei Gao, Xiaofei Zang, Bin Cai, and Yiming Zhu[b]
Shanghai Key Lab of Modern Optical System, Institute of Optical-Electrical Engineering and Engineering Research Center of Optical Instrument and System, Ministry of Education, University of Shanghai for Science and Technology, No. 516 JunGong Rd., Shanghai, China 200093

(Received 18 September 2013; accepted 1 December 2013; published online 17 December 2013)

To mechanically manipulate of electromagnetic induced transparency (EIT) in terahertz asymmetric parallel-plate waveguide cavities, the influence of waveguide spacing on the transmission response has been studied experimentally. After setting the appropriate shifting length between two cavities, we found with mechanically increasing the waveguide spacing, the symmetric resonance shows degeneracy when its wavelength is smaller than the waveguide spacing. An on-to-off modulation for symmetric resonance appeared in EIT can be observed with destructive interference broken. This control mechanism of EIT will open a door to design the tunable EIT devices. © *2013 AIP Publishing LLC*. [http://dx.doi.org/10.1063/1.4852115]

Electromagnetically induced transparency (EIT) is realized in atomic systems and results from coherently quantum interference.[1] Since excitation of an EIT in atomic systems demands low temperature environment, this realization has encouraged a continuous search for mimicking EIT in classical systems, such as coupled resonators,[2,3] metal-insulator-metal (MIM) plasmonic waveguides,[4,5] and metamaterial,[6–9] etc. For practical applications, a tunable EIT is more attractive than that of fixed one; therefore, numerous approaches for realizing this tunability have been reported. One of them was using optical pump beam to control the EIT effect in metamaterials.[9] A changing-over active manipulation of the EIT is demonstrated through adjusting of the dark mode in terahertz (THz) metamaterials, which can facilitate chip-scale THz active devices. Another example uses MIM structure, which can control the EIT effect by varying the geometrical parameters of the resonator.[4,5] While a MIM with cavities provides an ideal basic structure for achieving waveguide based EIT, however, high qualified complex nanofabrication is hardly achievable with existing fabrication technology.[5]

By exciting the transverse electromagnetic (TEM) mode, the parallel plate waveguide (PPWG) has been considerable interest concerned for its various of applications in THz regime.[10] Recently, the interest for studying the lowest-order transverse-electric mode (TE_1) in PPWG is increased due to its ultra-low loss and low distortion characteristics.[11] Recent progress has led to tremendous results including low-loss waveguide bends,[12] microfluidic sensor,[13,14] and reflector,[15] etc. In our previous work, the EIT effect was found based on PPWG-cavities system by varying the shifting length between two cavities.[16] In other words, the PPWG-cavities system includes the waveguide spacing as another degree of freedom, which has not been mentioned in Ref. 16. In this paper, in order to manipulate the EIT, we experimentally investigate the dependence of transmission response on the waveguide spacing between the two plates in the PPWG-cavities system. In the experiment, a cylindrical waveguide coupler is used to improve the coupling.[17] Experimental results show that as the EIT occurs, the symmetric and asymmetric resonances show red-shift with the increase of spacing. Furthermore, as the spacing is increased up to over the symmetric resonant wavelength, this resonance degenerates. Numerical simulations based on the Finite Element Method (Comsol Multiphysics) indicate that the symmetric resonance is a guided mode and results from strong destructive interference with the field in the cavity. Above the light line, another kind of guided mode is excited with the degeneracy of the symmetric resonance. This guided mode has weak interaction with two cavities and leads to high transmission. Comparing with EIT controlling realized by other methods, this manipulation has two features: (i) it provides a simpler method to tune waveguide-based EIT without any additional complex devices (for example, optical pump-terahertz probe measurements in Ref. 9); (ii) such mechanically tunibility is more convenient than those by varying the geometrical parameters in metamaterials[8] and MIM with cavities.[4] Our method can be applied to design slow light waveguide, microfluidic sensor and other tunable THz devices.

The geometry of the THz PPWG cavities used in our experiments is shown in Fig. 1. The total structure is comprised of two 20 mm length coupled parts and a 5 mm flat part. The cylindrical coupler of the PPWG has a 32 mm radius of curvature, 45 mm length, and 30 mm width, as shown in Fig. 1(a). The cylindrical coupler is a continuously changing surface which can remove the discontinue boundary, thereby the THz beam is adiabatically concentrated on the waveguide with the lower reflection loss. The two 5 mm wide (z-direction) and 3 mm length (x-direction) copper plates with micro-machined grooves (400 μm depth (h), 400 μm width (w)) are embedded into the flat area of the top and bottom plates. A z-direction polarized (TE) THz beam is focused into the coupled part. We covered the boundary between the groove sample plate and waveguide by using aluminum foils to avoid the imperfection in the waveguide. In the following experiments, the shifting length L is kept to 200 μm in order to obtain the obvious EIT effect.[16]

[a]Electronic mail: linchen@usst.edu.cn
[b]Electronic mail: ymzhu@usst.edu.cn

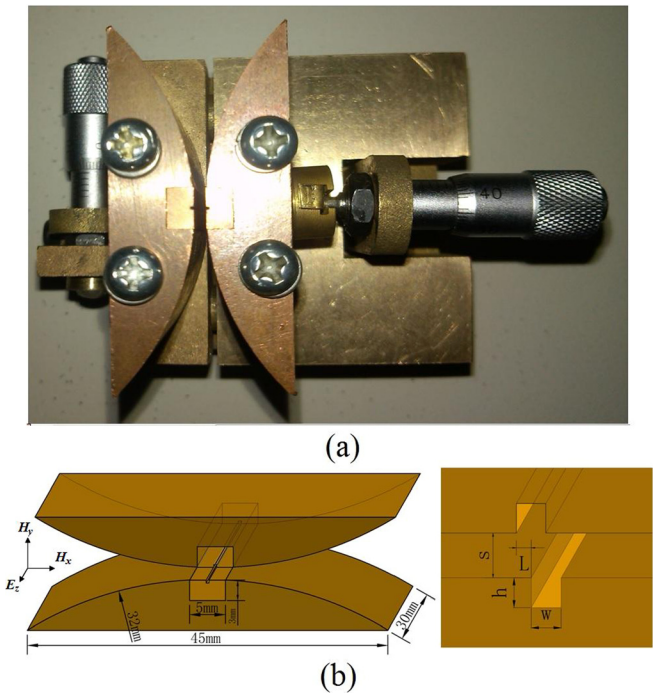

FIG. 1. (a) Copper sample (b) Geometry of cylindrical PPWG and cavity. W: the width of the groove; h: the depth of the groove; S: the waveguide spacing; and L: the shifting length between two grooves.

A combined fast and slow scan based THz time domain spectroscopy (THz-TDS) was used to measure the transmission spectra of PPWG.[16] A femtosecond fiber laser was applied to pump and detect THz wave, with the central wavelength at 780 nm, output power 150 mW, pulse duration around 90 fs, and repeat frequency at 80 MHz. We combine the fast scan with the slow scan to expand the overall delay line. After passing through slow delay line and fast delay line, the pump beam was introduced into the low-temperature-grown (LTG)-GaAs based photoconductive switch (THz emitter). The transmitted THz wave from the sample was detected by another LTG-GaAs based photoconductive switch (THz detector). We measured the time domain waveform of free space, PPWG, PPWG-cavities system with shifting length $L = 200\ \mu$m, as shown in Fig. 2. By combining the

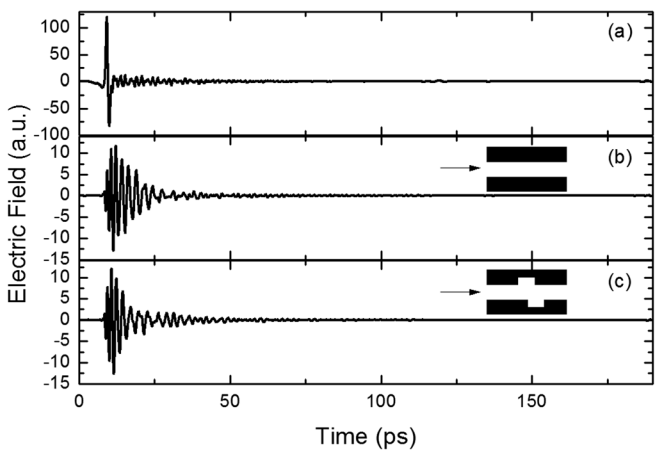

FIG. 2. Time scans corresponding to THz wave propagation through (a) free space, (b) PPWG with $S = 610\ \mu$m, (c) PPWG-cavities system with shifting length $L = 200\ \mu$m. Longitudinal cross-sections (along the direction of propagation) are shown inset.

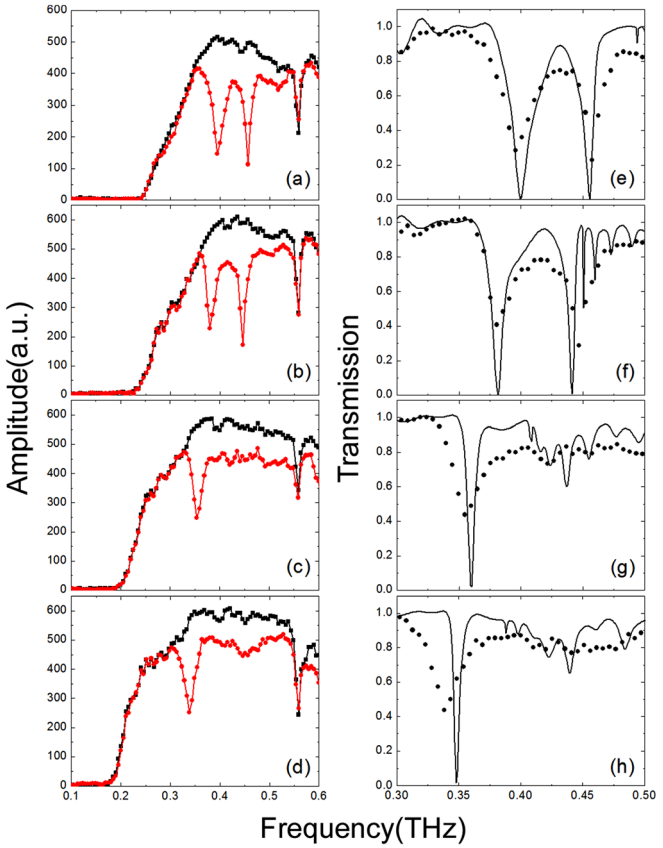

FIG. 3. (a)–(d) Measured THz spectra with various air gaps (a) $S = 610\ \mu$m, (b) $S = 670\ \mu$m, (c) $S = 740\ \mu$m, and (d) $S = 780\ \mu$m. The black and red lines indicate reference and output spectra. (e)–(h) Comparison of measured power transmission spectra (dots) and simulated power transmission (lines) for spectra Figs. 3(a)–3(d), respectively.

fast scan with slow optical delay line, the overall delay line can be expanded to 190 ps.

Then, four different waveguide spacings, with $S = 610$, 670, 740, and 780 μm, were used to study the characteristics of the EIT. Figures 3(a)–3(d) show the spectra of each measured THz pulse with waveguide spacings of 610, 670, 740, and 780 μm, respectively. The black and red curves indicate the PPWG spectra without cavities (Fourier-transforming the 190 ps time-scan of Fig. 2(b)) and the output spectra of PPWG cavities system with different S, respectively. Figs. 3(e)–3(h) show the experimental (dots) and simulation (black lines) power transmission by comparing the spectra of the propagated pulses with and without the cavities in Figs. 3(a)–3(d). The metal is set as a perfect electrical conductor in the simulation due to the disregard for the attenuation loss of the metal in the THz range. At least 3 more observations may be inferred by looking at Figs. 3(a)–3(h): (i) The amplitude spectrum (Figs. 3(a)–3(d)) exhibits a complete loss of spectral power up to the cutoff frequencies of 0.244, 0.236, 0.202, and 0.192 THz, corresponding to $S = 610$, 670, 740, and 780 μm, respectively.[11] The water-vapor absorption lines can also been found (0.557 THz) in Figs. 3(a)–3(d); (ii) As $S = 610\ \mu$m, the transmission show strong EIT effect, as described in Ref. 16. When S is increased from 610 μm to 780 μm, the low asymmetric resonance shows red-shift. The asymmetric resonant frequencies for $S = 610$, 670, 740, and 780 μm are 0.395, 0.379, 0.354, and 0.338 THz, respectively. This red-shift of high symmetric resonances can also be

found for $S = 610$ and $670\,\mu$m, where the resonant frequencies are 0.456 and 0.446 THz, respectively; (iii) As S is increased to $740\,\mu$m, the main symmetric resonance is degenerated in Figs. 3(c) and 3(g). This effect can also been found when S is equal to $780\,\mu$m. The measured and simulated results show good agreements. The deviation of experimental and numerical results is probably caused by the imperfections in the fabrication in real structures, which introduces further rearrangement of resonant frequencies.[16]

To understand the characteristic of the EIT change, in Fig. 4 we report the two dimensional transmission map for the PPWG cavities used in the measurement, obtained by varying incident frequency ν and waveguide spacing ($1/S$). In Fig. 4, the white line indicates the light line and the white dashed lines marked as "I," "II," "III," and "IV" stand for the waveguide spacings S of 610, 670, 740, and $780\,\mu$m ($1/S = 1.64$, 1.49, 1.35, and $1.28\,\text{mm}^{-1}$) in the experiment, respectively.

First, as mentioned above in experiment, when the waveguide spacing S decreases ($1/S$ increases), the symmetric and asymmetric resonant frequencies show red-shift. This red-shift effect is similar to the result of PPWG with single cavity for both TE[18] and TM[19] polarizations. The resonant frequency can be expressed as[19]

$$v(S) \propto \frac{c}{2 \times (2h_{eff} + S)}, \tag{1}$$

where c is the light velocity in vacuum ($3 \times 10^8\,\text{m/s} = 0.3$ THz/mm^{-1}) and h_{eff} is the effective cavity height. The value of h_{eff} for asymmetric resonance is not equal to that for symmetric resonance due to the electric field difference between two resonances at resonant frequencies (shown in Figs. 4(b) and 4(d) of Ref. 16). This process causes the red-shift of two resonances observed in both experiment and simulation. The mechanism of red-shift in PPWG-cavities system is identical to that of the single cavity;[18] the only difference is the single resonance supported by PPWG with one cavity and two different resonances supported by asymmetric PPWG cavities.

Moreover, as shown in Fig. 4, the high symmetric resonance of the PPWG cavities terminates at the point ($1.43\,\text{mm}^{-1}$, 0.43 THz) in light line (white line). The occurrence of the degeneracy can be obviously found for the symmetric resonance. In order to investigate the mechanism of such degeneracy, the electric field distributions E_z of points marked as "A" and "B" in Fig. 4 were shown in Figs. 5(a) and 5(b), respectively. The light line in Fig. 4 implies the condition $S = \lambda$, where λ represents incident THz wavelength. In both Figs. 5(a) and 5(b), the propagating THz beams indicate the guided mode property. In Fig. 5(b), the PPWG-cavities system shows the excellent confinement to the incident wave when the waveguide spacing S is smaller than the resonant wavelength of symmetric guided mode. We can clearly find the destructive interference with the field in two cavities in Fig. 5(b), which results in the low transmission at the output. The top (bottom) cavity in this case can be acted as a reflector and the incident wave has the strong interaction with two cavities. However, in Fig. 5(a), as S is larger than the wavelength of incident beam, another type of guided mode can be excited in the propagation direction of PPWG. The low energy in the cavity shows weaker interaction between the incident wave and two cavities than that in Fig. 5(b). As a result, the energy of such guided mode leaks through the exit side of the waveguide, followed by the high transmission in the forward direction. This guided mode is analogous to the guided propagating light beam in the traditional dielectric waveguide in visible range.[20,21] On the contrary, the lower asymmetric resonance can be observed in all experiment due to its value of frequency below the light line.

So far, we can describe the mechanism of manipulation of EIT in PPWG cavities system. By fixing appropriate

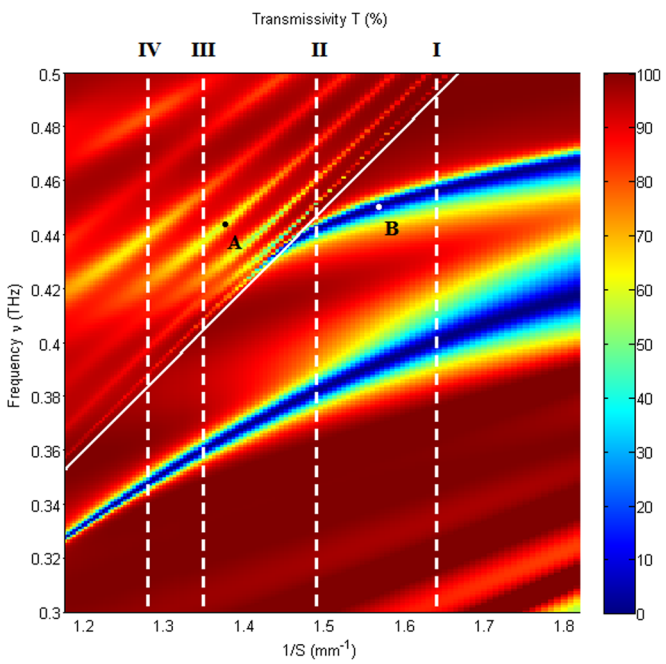

FIG. 4. The 2-dimension transmission map for two cavities with L = 200 μm. The white line indicates the light line. The white dashed lines are the examples in the experiment.

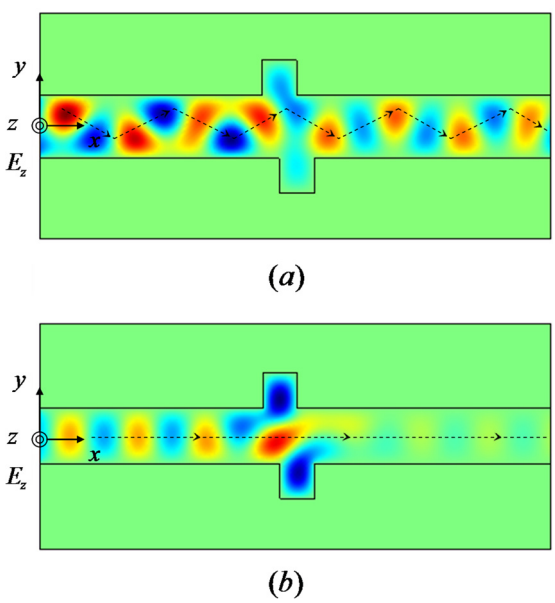

FIG. 5. The electric field distribution of structure at points marked as "A" and "B" in Fig. 4. The dashed lines indicate the propagating paths of electromagnetic wave for both conditions. (a) The electric field distribution of point "A." (b) The electric field distribution of point "B."

shifting length L (200 μm), as S increases and the two resonant wavelengths are larger than S (below the light line), EIT can be found obviously and the two resonances (including the transparent peak) show red-shift. Once the symmetric resonant wavelength is smaller than S, the incident THz wave interacts weakly with two cavities and propagates along the PPWG. Since the symmetric resonance appeared in EIT comes from the destructive interference with the field in two cavities, as the waveguide spacing increases, this interference is broken and an on-to-off modulation for symmetric resonance can be achieved in this process. The mechanism of above manipulation is different from control of EIT in metamaterial and plasmonics.[4,5,8,9] In addition, active electrical manipulation of EIT can also be achieved by using a piezo-actuator in order to adjust waveguide spacing using the voltage source.[19]

In conclusion, control of EIT in the PPWG cavities can be achieved by adjusting the waveguide spacing. By fixing the shifting length to achieve strong EIT, both symmetric and asymmetric resonances show red-shift with the increase of spacing. The symmetric resonance degenerates above the light line. An on-to-off control of the symmetric resonance appeared in EIT is achieved by mechanically properly tuning the spacing. It may inspire interest in developing mechanically tunable waveguide based EIT, resulting in a wide range of tunable compact THz devices, such as slow light components, sensitive sensors, and electromagnetically induced absorbers.

This work was partly supported by National Program on Key Basic Research Project of China (973 Program, 2014CB339806), Shanghai Basic Research Program (11ZR1425000), Basic Research Key Project (12JC1407100), Major National Development Project of Scientific Instrument and Equipment (2011YQ150021) (2012YQ14000504), the Key Scientific and Technological Project of Shanghai Municipality (12142200100), National Natural Science Foundation of China (11174207) (61138001) (61007059) (61205094) (61307126), and the Leading Academic Discipline Project of Shanghai Municipal Government (S30502).

[1]K. J. Boller, A. Imamoglu, and S. E. Harris, Phys. Rev. Lett. **66**, 2593 (1991).
[2]X. Zang and C. Jiang, J. Phys. B **43**, 065505 (2010).
[3]X. Zang, T. Zhou, B. Cai, and Y. Zhu, J. Opt. Soc. Am. B **30**, 1135–1140 (2013).
[4]Y. Huang, C. J. Min, and G. Veronis, Appl. Phys. Lett. **99**, 143117 (2011).
[5]Z. H. Han and S. I. Bozhevolnyi, Opt. Express **19**(4), 3251–3257 (2011).
[6]L. Chen, Y. M. Zhu, X. F. Zang, B. Cai, Z. Li, L. Xie, and S. L. Zhuang, Light Sci. Appl. **2**, e60 (2013).
[7]R. Singh, A. N. IAI, Y. P. Yang, D. R. Chowdhury, W. Cao, C. Rockstuhl, T. Ozaki, R. Morandotti, and W. L. Zhang, Appl. Phys. Lett. **99**, 201107 (2011).
[8]Z. Li, Y. Ma, R. Huang, R. Singh, J. Gu, Z. Tian, J. Han, and W. Zhang, Opt. Express **19**, 8912–8919 (2011).
[9]J. Q. Gu, R. Singh, X. J. Liu, X. Q. Zhang, Y. F. Ma, S. Zhang, S. A. Maier, Z. Tian, A. K. Azad, H. T. Chen, A. J. Taylor, J. G. Han, and W. L. Zhang, Nat. Commun. **3**, 1151 (2012).
[10]R. Mendis and D. Grischkowsky, Opt. Lett. **26**, 846–848 (2001).
[11]R. Mendis and D. M. Mittleman, Opt. Express **17**, 14839–14850 (2009).
[12]R. Mendis and D. M. Mittleman, Appl. Phys. Lett. **97**, 031106 (2010).
[13]R. Mendis, V. Astley, J. Liu, and D. M. Mittleman, Appl. Phys. Lett. **95**, 171113 (2009).
[14]V. Astley, K. S. Reichel, J. Jones, R. Mendis, and D. M. Mittleman, Appl. Phys. Lett. **100**(23), 231108 (2012).
[15]J. Liu, R. Mendis, and D. M. Mittleman, New J. Phys. **15**, 055002 (2013).
[16]L. Chen, C. Gao, J. Xu, X. Zang, B. Cai, and Y. Zhu, Opt. Lett. **38**, 1379–1381 (2013).
[17]M. Theuer, A. J. Shutler, S. Harsha, B. R. Sree, R. Beigang, and D. Grischkowsky, Appl. Phys. Lett. **98**(7), 071108 (2011).
[18]V. Astley, B. McCracken, R. Mendis, and D. M. Mittleman, Opt. Lett. **36**, 1452–1454 (2011).
[19]E. S. Lee and T. Jeon, Opt. Express **20**, 29605 (2012).
[20]L. Chen, Z. Q. Cao, F. Ou, H. G. Li, Q. S. Shen, and H. C. Qiao, Opt. Lett. **32**, 1432–1434 (2007).
[21]L. Chen, X. B. Liu, Z. Q. Cao, and S. L. Zhuang, J. Opt. **13**, 035002 (2011).